From Kinetic Instability to Bose-Einstein Condensation and Magnon Supercurrents

Alexander J. E. Kreil,[1,*] Dmytro A. Bozhko,[1] Halyna Yu. Musiienko-Shmarova,[1] Vitaliy I. Vasyuchka,[1] Victor S. L'vov,[2] Anna Pomyalov,[2] Burkard Hillebrands,[1] and Alexander A. Serga[1]

[1]*Fachbereich Physik and Landesforschungszentrum OPTIMAS, Technische Universität Kaiserslautern, 67663 Kaiserslautern, Germany*

[2]*Department of Chemical and Biological Physics, Weizmann Institute of Science, Rehovot 76100, Israel*

(Received 28 March 2018; published 15 August 2018)

Evolution of an overpopulated gas of magnons to a Bose-Einstein condensate and excitation of a magnon supercurrent, propelled by a phase gradient in the condensate wave function, can be observed at room temperature by means of the Brillouin light scattering spectroscopy in an yttrium iron garnet material. We study these phenomena in a wide range of external magnetic fields in order to understand their properties when externally pumped magnons are transferred towards the condensed state via two distinct channels: a multistage Kolmogorov-Zakharov cascade of the weak-wave turbulence or a one-step kinetic instability process. Our main result is that opening the kinetic instability channel leads to the formation of a much denser magnon condensate and to a stronger magnon supercurrent compared to the cascade mechanism alone.

DOI: 10.1103/PhysRevLett.121.077203

Bose-Einstein condensation (BEC) is a fascinating quantum phenomenon that manifests itself in the formation of a coherent macroscopic state from chaotic motions in a thermalized many-particle system. In spite of being a consequence of equilibrium Bose statistics [1,2], BEC can also occur in rather nonequilibrium systems, such as overpopulated gases of bosonic quasiparticles—excitons [3], polaritons [4–6], photons [7], and magnons [8–10]—as a result of local quasiequilibrium conditions near the minima of their frequency spectra. BEC formation in different quasiparticle systems constitutes a challenge of fundamental importance for physics in general and for possible applications in which BEC of quasiparticles is used for data processing. A particularly interesting case is given by a magnonic BEC [10,11] observed at room temperature in the low-damping ferrimagnetic material yttrium iron garnet (YIG, $Y_3Fe_5O_{12}$) [12]. Such a condensate is created from a magnon gas, overpopulated by intensive parametric injection of magnons [9]. The parametric magnons are then transferred by step-by-step cascade processes [13–16] down the frequency band, followed by a thermalization of low-energy magnons into the BEC state [9,11,17–20]. Under certain conditions, the cascade processes can be augmented by a direct transfer of the parametrically injected magnons to the lowest energy states [20,21]. In this case, referred to as a kinetic instability (KI) process [22,23], a dense cloud of noncoherent magnons is formed close to the BEC point. By the energy conservation law, the same number of parametric magnons is transferred to higher energy states and, thus, a strongly nonequilibrium magnon gas distribution, characterized by two population maxima, is formed.

In this Letter, we show experimentally and theoretically that KI provides favorable conditions for a more efficient magnon condensation and for a stronger BEC-related supercurrent spin transport [24] compared to the cascade-only scenario.

In our experiment, BEC formation is initiated by an external quasihomogeneous electromagnetic field of frequency ω_p that parametrically excites pairs of magnons with wave vectors $\pm\mathbf{q}_p$ and frequencies $\omega(\pm\mathbf{q}_p)$ via a three-wave decay process [25–27]

$$\omega_p = \omega(\mathbf{q}_p) + \omega(-\mathbf{q}_p) \Rightarrow \omega(\mathbf{q}_p) = \omega_p/2. \qquad (1)$$

At some threshold pumping power, the parametric magnon excitation compensates the natural magnon damping. A magnon mode that has the lowest damping frequency $\gamma(\mathbf{q}_p)$ and the strongest coupling to the pumping field starts growing exponentially in time.

Figure 1 illustrates the frequency spectrum $\omega(\mathbf{q})$ of magnons in an YIG film magnetized in plane by a bias magnetic field $\mathbf{H}$. The minimum of the spectrum is located at some wave vector $\mathbf{q} = \pm\mathbf{q}_{\min}$, where $\mathbf{q}_{\min} \| \mathbf{H}$. The parametrically pumped magnons are excited with $\mathbf{q}_p \perp \mathbf{H}$ and fill a part of the isofrequency "resonance" surface [Eq. (1)] [11,19,25]. It can be shown that nonlinear magnon scattering causes their transfer from this parametric excitation (PE) zone with the frequency $\omega_p/2$ toward the frequency well around $\omega_{\min}$ [28]. Afterwards, thermalization of the magnon occupation number distribution $n(\mathbf{q})$, local in phase space, can lead to the BEC of magnons at $\mathbf{q} = \mathbf{q}_{\min}$ [10].

There are two possible channels of the magnon transfer toward $\omega_{\min}$. The first one is a step-by-step flux of $n(\mathbf{q})$ [13]

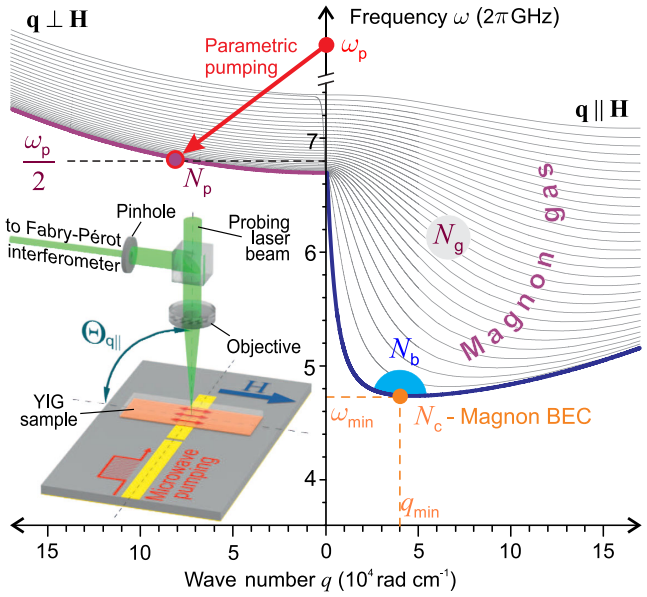

FIG. 1. Schematic view of the experimental setup. Magnon spectrum of a 5.6-μm-thick YIG film magnetized in plane by a bias magnetic field $H = 1700$ Oe shown for the wave vector $\mathbf{q}$ perpendicular (left part) and parallel (right part) to the applied field. The red arrow illustrates the process of parametric pumping. N_p = total number of parametrically excited magnons at $\omega_p/2$; N_c = number of BEC magnons at $\omega_c = \omega_{\min}$; N_b = number of gaseous magnons near $\omega_{\min}$ and $q_{\min}$; N_g = number of magnons in the parametrically overpopulated gas of magnons below $\omega_p/2$. (Inset) Sketch of the experimental setup. By using a resonance microstrip circuit, a pumping electromagnetic wave is delivered to the YIG sample and conditions of parallel parametric pumping are realized. The light inelastically scattered by magnons is analyzed by a Fabry-Perot interferometer. Wave-number-selective probing of magnons with wave vectors $\mathbf{q}\|\mathbf{H}$ is realized by varying the incidence angle $\Theta_{q_\parallel}$ between the field $\mathbf{H}$ and the probing laser beam [29].

(Kolmogorov-Zakharov cascade) similar to the Richardson-Kolmogorov cascade of the turbulent kinetic energy in classical hydrodynamic turbulence [30]. The second channel can arise from the KI process [17,18]. Here, a fusion of two parametrically injected magnons with $\omega(\mathbf{q}_p) \approx \omega(\mathbf{q}'_p) \approx \omega_p/2$ leads to the creation of two secondary magnons [a low-frequency magnon with $\omega(\mathbf{q}) \gtrsim \omega_{\min}$ and a high-frequency magnon with $\omega(\mathbf{q}') \simeq \omega_p - \omega_{\min}$] in the $2 \Leftrightarrow 2$ scattering process determined by the conservation laws

$$\omega_p = \omega(\mathbf{q}_p) + \omega(\mathbf{q}'_p) = \omega(\mathbf{q}) + \omega(\mathbf{q}'), \tag{2a}$$

$$\mathbf{q}_p + \mathbf{q}'_p = \mathbf{q} + \mathbf{q}'. \tag{2b}$$

These laws define the part of the resonance surface, or KI zone, for which the KI process is allowed.

In contrast to the dynamical process of the parametric instability, in which the strong phase correlation between three waves (photon and two magnons) plays a crucial role, the phase correlation between waves, involved in Eq. (2a) is very weak [25]. As a result, the magnon evolution in the KI process can be described in terms of their occupation numbers $n(\mathbf{q})$ in the framework of a kinetic equation [13,25] (hence the name [22]).

Parametric magnons, participating in the KI processes, cause a *negative* contribution $\gamma_{\mathrm{KI}} = -A\mathcal{N}_p^2 < 0$ to the original *positive* damping frequency of the bottom magnons γ_b, modifying their total damping frequency $\Gamma_p = \gamma_b - A\mathcal{N}_p^2$. Here $\mathcal{N}_p$ is the magnon number in the KI zone and A is a dimensional constant.

When $\mathcal{N}_p$ exceeds a critical value $\mathcal{N}_{\mathrm{cr}} = \sqrt{\gamma_b/A}$, the modified damping frequency Γ_b becomes negative [22] and the number of the gaseous low-frequency, or "bottom," magnons $N_b \propto \exp(-\Gamma_b t)$ grows exponentially. This phenomenon, suggested theoretically and discovered experimentally in Ref. [22], is inherent to systems of nonlinear waves to the same extent as the parametric instability and the Bose-Einstein condensation processes.

In the following, we compare the dynamics of the bottom magnons for different values of the external static bias magnetic field H, which determines the magnon frequency $\omega(H, \mathbf{q})$ in such a way that the KI channel is either allowed or forbidden by the conservation laws (2).

In our experiments, the magnons are injected in a 5.6-μm-thick in-plane magnetized YIG film at a frequency of $\omega_p/2 = 2\pi \times 6.8$ GHz by pulsed parametric pumping with a pulse length of 1 μs, repetition time 200 μs, and a peak power of 40 W. The time evolution of the magnon density is studied at room temperature by frequency-, time-, and wave-vector-resolved Brillouin light scattering (BLS) spectroscopy [11,29,31,32] (cf. Fig. 1). The detected BLS signal is proportional to the total number $N_{\mathrm{tot}} = N_b + N_c$ of gaseous and condensed magnons in the vicinity of $(\omega_{\min}, \mathbf{q}_{\min})$.

To illustrate the processes of magnon transfer to the bottom of the spectrum, we plot in Figs. 2(a)–2(c) the magnon scattering diagrams, representing the KI processes for three different values of H: (a) 1380, (b) 1700, and (c) 2000 Oe. Figure 2(d) shows the intensity of the BLS signals, which were collected from bottom magnons during the action of the parametric pumping, together with the threshold power of the parametric instability process, as functions of H.

Increasing the magnetic field shifts the frequency spectrum upward, changing the topology of the resonance surface $\omega(\mathbf{q}) = \omega_p/2$, as shown in Figs. 2(a)–2(c) by brown lines. At low H, it has almost elliptical shape [Fig. 2(a)], while at high H it is close to an "∞" shape [Fig. 2(c)]. Different topologies are delimited by $H_{\mathrm{cr}} \approx 1700$ Oe, corresponding to the minimum of the spectrum for $\mathbf{q}\perp\mathbf{H}$.

The parametric instability threshold and the distribution of parametric magnons on the resonance surface depend on its topology [25,33]. The magnons with $\mathbf{q}\perp\mathbf{H}$ have the largest coupling to the pumping field. Such magnons are

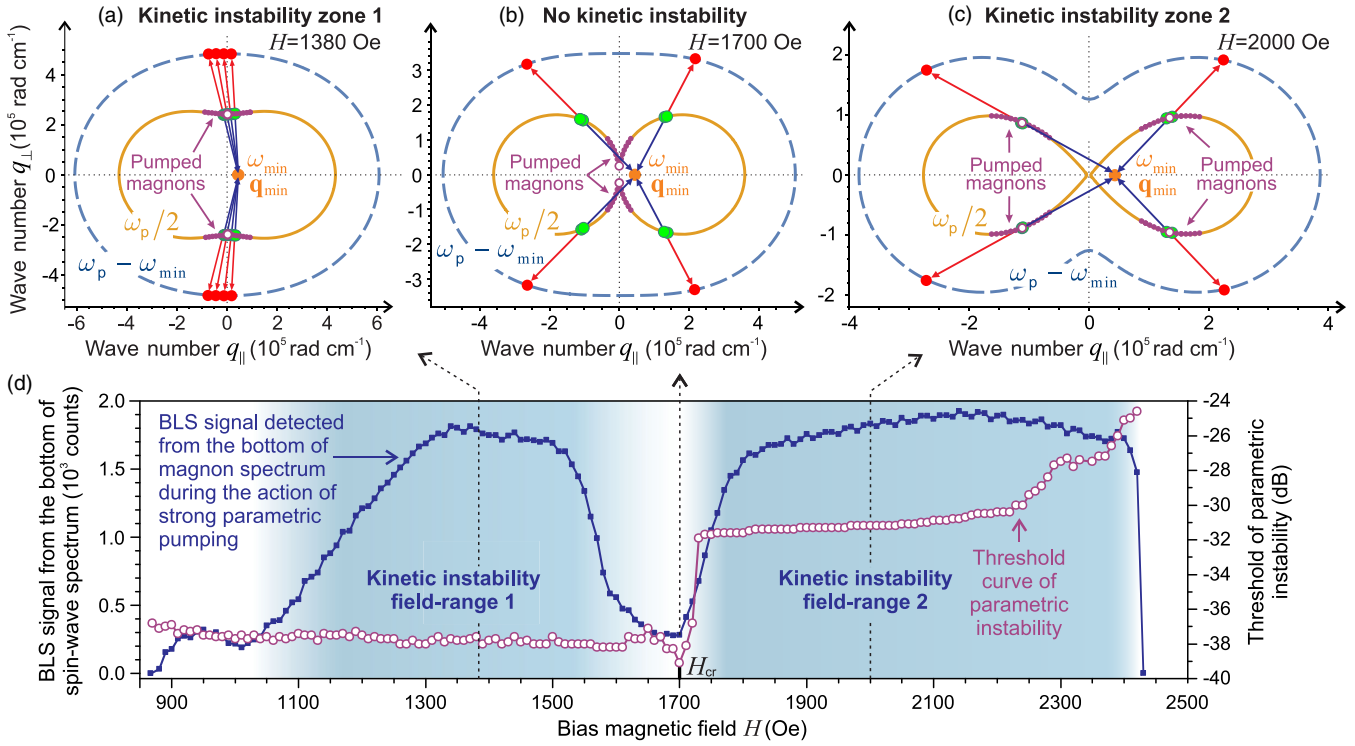

FIG. 2. (a)–(c) Diagrams describing the KI processes at different bias magnetic fields. The resonance surface $\omega(H, q_\parallel, q_\perp) = \omega_p/2$ of pumped magnons is shown in each panel by brown solid lines. The isofrequency surface $\omega(H, q_\parallel, q_\perp) = \omega_p - \omega_{\min}$ is shown by blue dashed lines. The BEC's spectral position at $(\omega_{\min}, \mathbf{q}_{\min})$ is indicated by the orange dot. The PE zones are marked by chains of magenta dots. The large empty magenta circles indicate spectral positions of magnons excited at the threshold of parametric instability. The parts of KI zones with $\mathbf{q}_p = \mathbf{q}'_p$, which mostly contribute to γ_{KI}, are denoted by green circles. The blue and red arrows illustrate the potentially possible scattering processes of magnons with $\mathbf{q}_p = \mathbf{q}'_p$ in the frequency band $\omega_p/2 \pm 2\pi \times 50$ MHz. (d) Measured BLS intensities of scattered magnons (blue squares) in comparison with the threshold curve of the parametric instability process (magenta empty circles). The shaded regions, in which KI processes are allowed by conservation laws, are marked as kinetic instability field range 1 and 2.

present on the resonance surface for $H \leq H_{\mathrm{cr}}$, but disappear for $H > H_{\mathrm{cr}}$. Accordingly, for $H \leq H_{\mathrm{cr}}$, the parametric instability threshold for magnons with $\mathbf{q} \perp \mathbf{H}$ [magenta empty circles in Fig. 2(d)] is almost constant and low. At high pumping powers, typical for our experiments, parametrically excited magnons are spread over the resonance surface around the $\mathbf{q} \perp \mathbf{H}$ line [25,33] as illustrated by chains of small magenta dots in Figs. 2(a) and 2(b).

For $H > H_{\mathrm{cr}}$, the frequency $\omega_p/2$ lies below the magnon branch $\mathbf{q} \perp \mathbf{H}$ (cf. Fig. 1) and the strongest coupled magnons are no longer present on the resonance surface. Therefore, the conditions of parametric excitation essentially change [34]. As a result, the parametric instability threshold sharply increases by about 6 dB, and the parametric magnons are excited on the resonance surface $\omega(\mathbf{q}) = \omega_p/2$ apart from $\mathbf{q}_\perp$ [25].

The PE and KI zones cover different parts of the resonance surface for different H. When these two zones overlap, the magnon number in the KI zone $\mathcal{N}_p$ approaches the total number of parametric magnons N_p. If the KI zone and the PE zone are well separated, $\mathcal{N}_p \ll N_p$. The comparison of the distribution of KI zones, obtained by detailed numerical analysis of Eqs. (1) and (2), with known PE zones [25] for different values of H, indicate the following. (i) KI and PE zones are well overlapping for $H < 1600$ Oe, denoted as the kinetic instability field range 1 in Fig. 2(d), and for $H > 1650$ Oe, denoted as kinetic instability field range 2. In both cases, we expect $\mathcal{N}_p \simeq N_p$, leading to high efficiency of the KI channel, as observed [two broad maxima on the curve with blue squares in Fig. 2(d)]. (ii) For intermediate values of $H \simeq H_{\mathrm{cr}}$, the KI and PE zones are well separated. In this case, we expect that $\mathcal{N}_p \ll N_p$ and KI processes are either strongly suppressed or forbidden, as it is evident from the deep minimum of the BLS intensity curve. Note that in both KI field ranges the number of BLS counts, which is proportional to $N_{\mathrm{tot}}(H)$, is on the order of 10^3, while it does not exceed 300 counts for H_{cr}. Thus, we conclude that the KI channel is at least an order of magnitude more efficient in the transfer of parametrically exited magnons to the bottom spectral area than the step-by-step Kolmogorov-Zakharov cascade.

The coherent condensed state, formed from the low-frequency magnons, may be evidenced by the detection

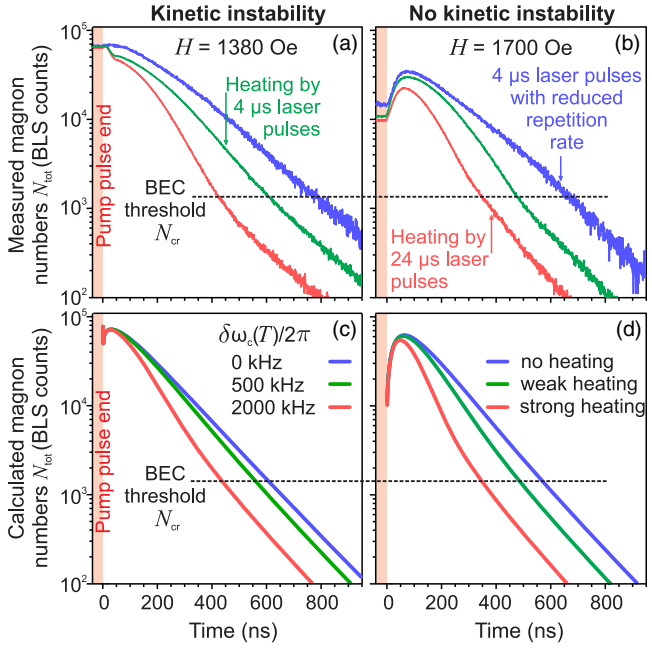

FIG. 3. Experimental and calculated dynamics of the total number of the bottom magnons N_{tot} influenced by a local heating of the YIG film. The BLS data are collected in a 150 MHz frequency band near the bottom of the magnon spectrum for different heating regimes in the first field range of kinetic instability (a) and at the critical bias field $H = H_c$ (b). The red, green, and blue curves represent strong, medium, and negligibly small local heating, respectively. (c),(d) Theoretical dependencies of the magnon densities, calculated taking into account different temperature-dependent shifts $\delta\omega_c(T)$ of the BEC frequency using the model from [24] with the initial conditions corresponding to the cases with and without KI. Note, that the measured BLS signals are proportional to N_{tot}. The calculated curves were adjusted to give the same number of BLS counts at the end of the pump pulse ($t = 0$) as the experimental signals. The quantities of BLS counts in this experiment significantly exceed the numbers shown in Fig. 2(d) due to much longer data acquisition time.

of a magnon supercurrent excited by a local heating of the YIG film [24]. Given the efficiency of the KI channel in creating the overpopulated magnon gas at the bottom frequency area, one can expect it to affect the properties of both the BEC and the supercurrent. To study this influence, we compare the free evolution of a magnon BEC after the termination of the parametric pumping pulse under different local heating conditions. To control the heating, we use a pulsed laser focused onto the sample. The sample is probed by the same laser light, synchronized with the microwave pumping pulses [24]. The temperature of the probing BLS point is changed by adjusting the duration and the repetition rate of probing laser pulses.

The magnon decay dynamics is shown in Fig. 3 for $H = 1380$ Oe, corresponding to the KI field range 1, and for $H = 1700$ Oe, where KI is negligible. The main differences in the initial stages of the BLS signal evolution between these cases is the total number of bottom magnons observed just before the termination of the pumping pulse: $N_{\mathrm{tot}} \simeq 10^5$ BLS counts with KI in Fig. 3(a) and $N_{\mathrm{tot}} \simeq 10^4$ BLS counts without KI in Fig. 3(b). However, in the latter case, the BLS signal additionally increases in the course of the pumping-free evolution of the magnon system.

To understand this difference, we note that the cascade process creates a gradually decreasing distribution of the magnons between the resonance surface and the magnon spectrum bottom. After the pumping pulse ends, these magnons move to the minimum energy state by means of nonlinear four-magnon scattering and form there a pronounced delayed peak of the magnon gas density [11], clearly visible in Fig. 3(b). In contrast, the KI process strongly populates spectral states near ω_{min} already during the pumping pulse, as it is observed by BLS. The following redistribution of these magnons between the gaseous and BEC states does not change N_{tot} and thus is not reflected in the BLS dynamics.

Nevertheless, with or without KI, the heating of the probing point by a probing laser pulse leads to an enhanced signal decay at high magnon densities $N_{\mathrm{tot}}(t)$. This phenomenon, understood as a supercurrent-related outflow of condensed magnons from the heated probing spot [24], serves as a signature of the spontaneously established coherent magnon phase—the magnon BEC, independent of the magnon transfer scenario [35]. Figures 3(a) and 3(b) show that the supercurrent is not induced in experiments with a space-homogeneous cold film (reduced repetition rate, short laser pulse of 4 μs duration, blue lines), become noticeable for moderate local heating (high repetition rate, short laser pulse, green lines), and is pronounced for strong heating (high repetition rate, long laser pulse of 24 μs duration, red lines). At the later stage of the decay, when the BEC already disappeared and no phase coherency can be assumed in the magnon gas, the supercurrent vanishes in all cases.

To further understand the observed density evolution, we consider three groups of magnons: the magnon BEC group $N_c(t)$, the nearby bottom magnons group $N_b(t)$, and the gaseous magnons group $N_g(t)$ occupying the remaining part of the (ω, q) plane (see Fig. 1). The density dynamics of these magnons may be studied using the phenomenological model developed in Ref. [24]. The model uses the same magnon relaxation frequencies $\gamma_g = \gamma_b = \gamma_c$ for all three groups, a phenomenological parameter N_{cr} representing the threshold of Bose-Einstein condensation, and a supercurrent term describing the outflow of coherent magnons from the hot spot with temperature T to the cold part of the film with temperature T_0. It is assumed that the supercurrent is driven by a phase difference in the BEC wave function, created by the thermally induced change of the saturation magnetization that leads to a frequency shift $\delta\omega_c(T) = \omega_{\mathrm{min}}(T) - \omega_{\mathrm{min}}(T_0)$ between the hot and cold parts of the magnon condensate. In the current Letter,

the presence of the KI process is taken into account by a tenfold increase of the initial density in the bottom magnons group $N_b(t)$ in accordance with the experimental BLS data shown in Fig. 3(a). The simulation results presented in Figs. 3(c) and 3(d) clearly reproduce two distinct stages of the $N_{\mathrm{tot}}(t)$ evolution in the hot spot: a fast initial decay followed by a slower gradual decrease. Therefore, we firmly associate the enhancement of the initial decay, observed in our KI experiments, with the temperature-induced supercurrent of the magnon BEC [24].

To summarize, parametric pumping of magnons in YIG films creates a magnon BEC in a wide range of bias magnetic fields. At the same time, the formation of the magnon condensate is significantly intensified when kinetic instability processes are allowed. A narrow intense peak in the population of stochastic magnons, created via this process near the bottom of the magnon spectrum, serves as an efficient precursor for the BEC formation. Consequently, the resulting BEC state is denser by an order of magnitude compared to the one created under conditions when only Kolmogorov-Zakharov cascade spectral transfer is allowed. The existence of the magnon condensate is evidenced by our observation of a two-stage decay of a BEC-related BLS signal after the termination of the parametric pumping. Furthermore, a magnon supercurrent, responsible for this two-stage decay, is stronger in the KI case. We assert that the KI process, being a general physical phenomenon inherent for the systems of nonlinear waves, may be found in overpopulated gases of bosonic quasiparticles of a different nature, thus opening novel directions of research.

Financial support by the European Research Council within the Advanced Grant No. 694709 "SuperMagnonics" and by Deutsche Forschungsgemeinschaft (DFG) within the Transregional Collaborative Research Center SFB/TR 49 "Condensed Matter Systems with Variable Many-Body Interactions" as well as by the DFG Project No. INST 248/178-1 is gratefully acknowledged.

*kreil@rhrk.uni-kl.de

[1] A. Einstein, Quantentheorie des einatomigen idealen gases, Sitz. Ber. Preuss. Akad. Wiss. Phys. **22**, 261 (1924).

[2] A. Einstein, Quantentheorie des einatomigen idealen gases, Zweite Abhandlung, Sitz. Ber. Preuss. Akad. Wiss. Phys. **23**, 3 (1925).

[3] L. V. Butov, A. L. Ivanov, A. Imamoglu, P. B. Littlewood, A. A. Shashkin, V. T. Dolgopolov, K. L. Campman, and A. C. Gossard, Stimulated Scattering of Indirect Excitons in Coupled Quantum Wells: Signature of a Degenerate Bose-Gas of Excitons, Phys. Rev. Lett. **86**, 5608 (2001).

[4] J. Kasprzak, M. Richard, S. Kundermann, A. Baas, P. Jeambrun, J. M. J. Keeling, F. M. Marchetti, M. H. Szymańska, R. André, J. L. Staehli, V. Savona, P. B. Littlewood, B. Deveaud, and Le Si Dang, Bose-Einstein condensation of exciton polaritons, Nature (London) **443**, 409 (2006).

[5] R. Balili, V. Hartwell, D. Snoke, L. Pfeiffer, and K. West, Bose-Einstein condensation of microcavity polaritons in a trap, Science **316**, 1007 (2007).

[6] S. R. K. Rodriguez, J. Feist, M. A. Verschuuren, F. J. Garcia Vidal, and J. Gómez Rivas, Thermalization and Cooling of Plasmon-Exciton Polaritons: Towards Quantum Condensation, Phys. Rev. Lett. **111**, 166802 (2013).

[7] J. Klaers, J. Schmitt, F. Vewinger, and M. Weitz, Bose-Einstein condensation of photons in an optical microcavity, Nature (London) **468**, 545 (2010).

[8] A. S. Borovik-Romanov, Yu. M. Bun'kov, V. V. Dmitriev, and Yu. M. Mukharskiĭ, Long-lived induction signal in superfluid ^{3}He-B, JETP Lett. **40**, 1033 (1984); http://www.jetpletters.ac.ru/ps/1257/article_19014.shtml.

[9] Yu. D. Kalafati and V. L. Safonov, Possibility of Bose condensation of magnons excited by incoherent pump, JETP Lett. **50**, 149 (1989); http://www.jetpletters.ac.ru/ps/1126/article_17065.shtml.

[10] S. O. Demokritov, V. E. Demidov, O. Dzyapko, G. A. Melkov, A. A. Serga, B. Hillebrands, and A. N. Slavin, Bose-Einstein condensation of quasi-equilibrium magnons at room temperature under pumping, Nature (London) **443**, 430 (2006).

[11] A. A. Serga, V. S. Tiberkevich, C. W. Sandweg, V. I. Vasyuchka, D. A. Bozhko, A. V. Chumak, T. Neumann, B. Obry, G. A. Melkov, A. N. Slavin, and B. Hillebrands, Bose-Einstein condensation in an ultra-hot gas of pumped magnons, Nat. Commun. **5**, 3452 (2014).

[12] V. Cherepanov, I. Kolokolov, and V. L'vov, The saga of YIG: Spectra, thermodynamics, interaction and relaxation of magnons in a complex magnet, Phys. Rep. **229**, 81 (1993).

[13] V. E. Zakharov, V. S. L'vov, and G. E. Falkovich, *Kolmogorov Spectra of Turbulence (Wave Turbulence)* (Springer, New York, 1992).

[14] V. E. Demidov, O. Dzyapko, M. Buchmeier, T. Stockhoff, G. Schmitz, G. A. Melkov, and S. O. Demokritov, Magnon Kinetics and Bose-Einstein Condensation Studied in Phase Space, Phys. Rev. Lett. **101**, 257201 (2008).

[15] J. Hick, T. Kloss, and P. Kopietz, Thermalization of magnons in yttrium-iron garnet: Nonequilibrium functional renormalization group approach, Phys. Rev. B **86**, 184417 (2012).

[16] D. A. Bozhko, P. Clausen, A. V. Chumak, Yu. V. Kobljanskyj, B. Hillebrands, and A. A. Serga, Formation of Bose-Einstein magnon condensate via dipolar and exchange thermalization channels, Low Temp. Phys. **41**, 801 (2015).

[17] A. V. Chumak, G. A. Melkov, V. E. Demidov, O. Dzyapko, V. L. Safonov, and S. O. Demokritov, Bose-Einstein Condensation of Magnons under Incoherent Pumping, Phys. Rev. Lett. **102**, 187205 (2009).

[18] V. L. Safonov, *Nonequilibrium Magnons: Theory, Experiment, and Applications* (Wiley-VCH, New York, 2013).

[19] P. Clausen, D. A. Bozhko, V. I. Vasyuchka, B. Hillebrands, G. A. Melkov, and A. A. Serga, Stimulated thermalization of a parametrically driven magnon gas as a prerequisite for Bose-Einstein magnon condensation, Phys. Rev. B **91**, 220402(R) (2015).

[20] D. V. Slobodianiuk and O. V. Prokopenko, Kinetics of strongly nonequilibrium magnon gas leading to Bose-Einstein condensation, J. Nano-Electron. Phys. **9**, 03033 (2017).
[21] G. A. Melkov, V. L. Safonov, A. Y. Taranenko, and S. V. Sholom, Kinetic instability and Bose condensation of nonequilibrium magnons, J. Magn. Magn. Mater. **132**, 180 (1994).
[22] A. V. Lavrinenko, V. S. L'vov, G. A. Melkov, and V. B. Cherepanov, "Kinetic" instability of a strongly nonequilibrium system of spin waves and tunable radiation of a ferrite, Sov. Phys. JETP **54**, 542 (1981); http://www.jetp.ac.ru/cgi-bin/e/index/e/54/3/p542?a=list.
[23] G. A. Melkov and S. V. Sholom, Kinetic instability of spin waves in thin ferrite films, Sov. Phys. JETP **72**, 341 (1991); http://www.jetp.ac.ru/cgi-bin/e/index/e/72/2/p341?a=list.
[24] D. A. Bozhko, A. A. Serga, P. Clausen, V. I. Vasyuchka, F. Heussner, G. A. Melkov, A. Pomyalov, V. S. L'vov, and B. Hillebrands, Supercurrent in a room temperature Bose-Einstein magnon condensate, Nat. Phys. **12**, 1057 (2016).
[25] V. S. L'vov, *Wave Turbulence under Parametric Excitations (Applications to Magnetics)* (Springer, New York, 1994).
[26] A. G. Gurevich and G. A. Melkov, *Magnetization Oscillations and Waves* (CRC Press, Boca Raton, 1996).
[27] V. I. Vasyuchka, A. A. Serga, C. W. Sandweg, D. V. Slobodianiuk, G. A. Melkov, and B. Hillebrands, Explosive Electromagnetic Radiation by the Relaxation of a Multimode Magnon System, Phys. Rev. Lett. **111**, 187206 (2013).
[28] Y. M. Bunkov, E. M. Alakshin, R. R. Gazizulin, A. V. Klochkov, V. V. Kuzmin, V. S. L'vov, and M. S. Tagirov, High-T_c Spin Superfluidity in Antiferromagnets, Phys. Rev. Lett. **108**, 177002 (2012).
[29] C. W. Sandweg, M. B. Jungfleisch, V. I. Vasyuchka, A. A. Serga, P. Clausen, H. Schultheiss, B. Hillebrands, A. Kreisel, and P. Kopietz, Wide-range wave vector selectivity of magnon gases in Brillouin light scattering spectroscopy, Rev. Sci. Instrum. **81**, 073902 (2010).
[30] U. Frisch, *Turbulence: The Legacy of A.N. Kolmogorov* (Cambridge University Press, Cambridge, England, 1995).
[31] O. Büttner, M. Bauer, S. O. Demokritov, B. Hillebrands, Y. S. Kivshar, V. Grimalsky, Y. Rapoport, and A. N. Slavin, Linear and nonlinear diffraction of dipolar spin waves in yttrium iron garnet films observed by space- and time-resolved Brillouin light scattering, Phys. Rev. B **61**, 11576 (2000).
[32] A. A. Serga, C. W. Sandweg, V. I. Vasyuchka, M. B. Jungfleisch, B. Hillebrands, A. Kreisel, P. Kopietz, and M. P. Kostylev, Brillouin light scattering spectroscopy of parametrically excited dipole-exchange magnons, Phys. Rev. B **86**, 134403 (2012).
[33] V. V. Zautkin, V. S. L'vov, and S. L. Musher, Proof of stage-by-stage excitation of parametric spin waves, JETP Lett. **14**, 206 (1971).
[34] T. Neumann, A. A. Serga, V. I. Vasyuchka, and B. Hillebrands, Field-induced transition from parallel to perpendicular parametric pumping for a microstrip transducer, Appl. Phys. Lett. **94**, 192502 (2009).
[35] Y. M. Bunkov and V. L. Safonov, Magnon condensation and spin superfluidity, J. Magn. Magn. Mater. **452**, 30 (2018).